J|A|C|S ARTICLES

Published on Web 07/14/2010

A Combined Experimental and Theoretical Study of Ion Solvation in Liquid *N*-Methylacetamide

Haibo Yu,[†] Christopher L. Mazzanti,[‡] Troy W. Whitfield,[¶,||] Roger E. Koeppe II,[‡] Olaf S. Andersen,[§] and Benoît Roux*[,†,¶]

Department of Biochemistry and Molecular Biology, University of Chicago, 929 East 57th Street, Chicago, Illinois 60637, Department of Chemistry and Biochemistry, University of Arkansas, Fayetteville, Arkansas 72701, Biosciences Division, Argonne National Laboratory, 9700 South Cass Avenue, Argonne, Illinois 60649, and Department of Physiology and Biophysics, Weill Cornell Medical College, 1300 York Avenue, New York, New York 10065

Received April 18, 2010; E-mail: roux@uchicago.edu

Abstract: Most current biomolecular simulations are based on potential energy functions that treat the electrostatic energy as a sum of pairwise Coulombic interactions between effective fixed atomic charges. This approximation, in which many-body induced polarization effects are included in an average way, is expected to be satisfactory for a wide range of systems, but less accurate for processes involving the transfer and partition of ions among heterogeneous environments. The limitations of these potential energy functions are perhaps most obvious in studies of ion permeation through membrane channels. In many cases, the pore is so narrow that the permeating ion must shed most of its surrounding water molecules and the large energetic loss due to dehydration must be compensated by coordination with protein atoms. Interactions of cations with protein backbone carbonyl oxygens, in particular, play a critical role in several important biological channels. As a first step toward meeting the challenge of developing an accurate explicit accounting for induced polarization effects, the present work combines experiments and computation to characterize the interactions of alkali and halide ions with *N*-methylacetamide chosen to represent the peptide bond. From solubility measurements, we extract the solvation free energies of KCl and NaCl in liquid *N*-methylacetamide. Polarizable models based on the Drude oscillator are then developed and compared with available experimental and *ab initio* data. The good agreement for a range of structural and thermodynamic properties in the gas and condensed phases suggests that the polarizable models provide an accurate representation of ion−amide interactions in biological systems.

Introduction

Understanding the microscopic factors controlling the passage of ions through narrow molecular pores using molecular dynamics (MD) simulations remains a challenge. The large hydration energy of the ions contrasts with the small free energy barriers necessary for the fast ion conduction observed experimentally, implying that ion−protein association is ultimately controlled by a delicate balance of very strong interactions. Frequently, the permeation process involves the partial dehydration of an ion, followed by the translocation through the interior of a proteinaceous environment.[1] This archetype is well illustrated by the crystal structure of the KcsA channel. The pore of the KcsA channel comprises a wide aqueous vestibular entryway, lined by nonpolar residues on the intracellular side, leading up on the extracellular side to a narrow region lined by backbone carbonyl oxygens.[2] This region of the pore, formed by the residues corresponding to the signature sequence TTVGYG common to all K^+ channels,[3] acts as a "selectivity filter" by allowing only the passage of nearly dehydrated K^+ ions across the cell membrane. Such fundamental characteristics of ion conduction through narrow pores are also exemplified by the gramicidin A channel (gA),[4−7] where tight interactions between the permeating ion and the protein are critical. In such narrow molecular pores, a permeating ion must shed most of its surrounding water molecules, and the large energetic loss due to dehydration must be compensated by coordination with the backbone carbonyl oxygens.

[†] Department of Biochemistry and Molecular Biology, University of Chicago.
[‡] Department of Chemistry and Biochemistry, University of Arkansas.
[¶] Biosciences Division, Argonne National Laboratory.
[§] Department of Physiology and Biophysics, Weill Cornell Medical College.
[||] Current address: Program in Bioinformatics and Integrative Biology, University of Massachusetts Medical School, Worcestor, Massachusetts, 01605.

(1) Hille, B. *Ionic Channels of Excitable Membranes*, 3rd ed.; Sinauer: Sunderland MA, 2001.
(2) Doyle, D. A.; Cabral, J. a. M.; Pfuetzner, R. A.; Kuo, A.; Gulbis, J. M.; Cohen, S. L.; Chait, B. T.; MacKinnon, R. *Science* **1998**, *280*, 69–77.
(3) Heginbotham, L.; Abramson, T.; MacKinnon, R. *Science* **1992**, *258*, 1152–1155.
(4) Arseniev, A. S.; Barsukov, I. L.; Bystrov, V. F.; Lomize, A. L.; Ovchinnikov, Y. A. *FEBS Lett.* **1985**, *186*, 168–174.
(5) Ketchem, R. R.; Hu, W.; Cross, T. A. *Science* **1993**, *261*, 1457–1460.
(6) Ketchem, R. R.; Roux, B.; Cross, T. A. *Structure* **1997**, *5*, 1655–1669.
(7) Townsley, L. E.; Tucker, W. A.; Sham, S.; Hinton, J. F. *Biochemistry* **2001**, *40*, 11676–11686.

Meaningful MD simulation studies of ion permeation and ion selectivity in membrane channels must be based on force fields that provide a realistic and accurate representation of the microscopic interactions. A force field is a set of simple differentiable mathematical functions, parametrized to "mimic" the quantum mechanical Born−Oppenheimer energy surface. To enable the rapid calculation of the forces acting on atoms and molecules, the force fields currently used in most MD simulations of biomolecular systems represent the electrostatic energy as a sum of pairwise Coulombic interactions between fixed effective point charges attributed to each atom.[8−11] Such models, however, neglect the distortion of the electron density around an atom or molecule under the influence of an external field. The assumption is that many-body polarization effects are either negligible or can be accounted for in an average effective way by adjusting the atomic partial charges.[12] Whereas this approximation can yield useful results on a wide range of biomolecular systems of great complexity,[13−17] its ability to provide a quantitative description of processes involving the association of ions with proteins is necessarily limited. These problems are clearly illustrated by considering the thermodynamic solvation properties and the interaction of an ion with an isolated water or *N*-methylacetamide molecule.[18] Nonpolarizable force fields can reproduce both the hydration free energy and the ion−water dimer fairly accurately with a water dipole moment, that is larger than the experimental gas-phase value.[19−27] In contrast, it is not possible to construct an effective nonpolarizable model that is quantitatively accurate for both the solvation free energy and the ion−amide dimer interactions.[18] Such limitations are observed with the widely used biomolecular force fields, e.g., AMBER,[8] CHARMM PARAM27,[9] and GROMOS.[10] It is anticipated that including effects associated with induced electronic polarization explicitly in the force field can provide a more realistic microscopic description of such interactions,[14,18,28−35] and the development of accurate models is the object of much interest.[14,30,36,37] Current computational strategies include models based on induced dipoles,[38−47] fluctuating charges,[48−56] and classical Drude oscillators[57−61] (sometimes referred to as the Shell model,[62,63] or Charge-on-Spring[30,64,65]). Recent work also includes polarizable models going beyond the classical force field and adopting an electronic structure-based approach.[66,67] Models based on the classical Drude oscillator are particularly advantageous because they preserve the functional form of charge−charge interactions and

(8) Cornell, W. D.; Cieplak, P.; Bayly, C. I.; Gould, I. R.; Merz, K. M.; Ferguson, D. M.; Spellmeyer, D. C.; Fox, T.; Caldwell, J. W.; Kollman, P. A. *J. Am. Chem. Soc.* **1995**, *117*, 5179–5197.
(9) MacKerell, A. D.; et al. *J. Phys. Chem. B* **1998**, *102*, 3586–3616.
(10) Oostenbrink, C.; Villa, A.; Mark, A. E.; van Gunsteren, W. F. *J. Comput. Chem.* **2004**, *25*, 1656–1676.
(11) Jorgensen, W.; Maxwell, D.; Tirado-Rives, J. *J. Am. Chem. Soc.* **1996**, *118*, 11225–11236.
(12) Brooks, C. L.; Karplus, M.; Pettitt, B. M. *Proteins: A Theoretical Perspective of Dynamics, Structure, and Thermodynamics*; John Wiley & Sons: New York, 1988; Vol. LXXI.
(13) Karplus, M.; McCammon, J. A. *Nat. Struct. Biol.* **2002**, *9*, 646–652.
(14) Ponder, J. W.; Case, D. A. *Adv. Protein Chem.* **2003**, *66*, 27–85.
(15) van Gunsteren, W. F.; et al. *Angew. Chem., Int. Ed.* **2006**, *45*, 4064–4092.
(16) Jorgensen, W. L.; Tirado-Rives, J. *Proc. Natl. Acad. Sci. U.S.A.* **2005**, *102*, 6665–6670.
(17) Adcock, S. A.; McCammon, J. A. *Chem. Rev.* **2006**, *106*, 1589–1615.
(18) Roux, B.; Bernèche, S. *Biophys. J.* **2002**, *82*, 1681–1684.
(19) Berendsen, H. J. C.; Postma, J. P. M.; van Gunsteren, W. F.; Hermans, J. In *Intermolecular Forces*; Pullman, B., Ed.; Reidel: Dordrecht, 1981; p 331.
(20) Jorgensen, W. L.; Chandrasekhar, J.; Madura, J. D.; Impey, R. W.; Klein, M. L. *J. Chem. Phys.* **1983**, *79*, 926–935.
(21) Åqvist, J. *J. Phys. Chem.* **1990**, *94*, 8021–8024.
(22) Beglov, D.; Roux, B. *J. Chem. Phys.* **1994**, *100*, 9050–9063.
(23) Roux, B. *Biophys. J.* **1996**, *71*, 3177–3185.
(24) Jensen, K. P.; Jorgensen, W. L. *J. Chem. Theory Comput.* **2006**, *2*, 1499–1509.
(25) Joung, I. S.; Cheatham, T. E. *J. Phys. Chem. B* **2008**, *112*, 9020–9041.
(26) Joung, I. S.; Cheatham, T. E. *J. Phys. Chem. B* **2009**, *113*, 13279–13290.
(27) Carlsson, J.; Åqvist, J. *J. Phys. Chem. B* **2009**, *113*, 10255–10260.
(28) Cieplak, P.; Kollman, P. A. *J. Chem. Phys.* **1990**, *92*, 6761–6767.
(29) Roux, B. *Chem. Phys. Lett.* **1993**, *212*, 231–240.
(30) Yu, H. B.; van Gunsteren, W. F. *Comput. Phys. Commun.* **2005**, *172*, 69–85.
(31) Grossfield, A.; Ren, P. Y.; Ponder, J. W. *J. Am. Chem. Soc.* **2003**, *125*, 15671–15682.
(32) Jiao, D.; King, C.; Grossfield, A.; Darden, T.; Ren, P. *J. Phys. Chem. B* **2006**, *110*, 18553–18559.
(33) Lamoureux, G.; Roux, B. *J. Phys. Chem. B* **2006**, *110*, 3308–3322.
(34) Whitfield, T. W.; Varma, S.; Harder, E.; Lamoureux, G.; Rempe, S. B.; Roux, B. *J. Chem. Theory Comput.* **2007**, *3*, 2068–2082.
(35) Lopes, P. E. M.; Roux, B.; MacKerell, A. D. *Theor. Chem. Acc.* **2009**, *124*, 11–28.
(36) Rick, S. W.; Stuart, S. J. *Rev. Comput. Chem.* **2002**, 89–146.
(37) Jorgensen, W. L. *J. Chem. Theory Comput.* **2007**, *3*, 1877–1877.
(38) Barnes, P.; Finney, J. L.; Nicholas, J. D.; Quinn, J. E. *Nature* **1979**, *282*, 459–464.
(39) Goodfellow, J. M. *Proc. Nat. Acad. Sci. U.S.A.* **1982**, *79*, 4977–4979.
(40) van Belle, D.; Couplet, I.; Prevost, M.; Wodak, S. J. *J. Mol. Biol.* **1987**, *198*, 721–735.
(41) Sprik, M.; Klein, M. L. *J. Chem. Phys.* **1988**, *89*, 7556–7560.
(42) Caldwell, J.; Dang, L. X.; Kollman, P. A. *J. Am. Chem. Soc.* **1990**, *112*, 9144–9147.
(43) Wallqvist, A.; Berne, B. J. *J. Phys. Chem.* **1993**, *97*, 13841–13851.
(44) Bernardo, D. N.; Ding, Y. B.; Kroghjespersen, K.; Levy, R. M. *J. Phys. Chem.* **1994**, *98*, 4180–4187.
(45) Dang, L. X. *J. Phys. Chem. B* **1998**, *102*, 620–624.
(46) Gresh, N.; Cisneros, G. A.; Darden, T. A.; Piquemal, J. P. *J. Chem. Theory Comput.* **2007**, *3*, 1960–1986.
(47) Ponder, J. W.; Wu, C. J.; Ren, P. Y.; Pande, V. S.; Chodera, J. D.; Schnieders, M. J.; Haque, I.; Mobley, D. L.; Lambrecht, D. S.; DiStasio, R. A.; Head-Gordon, M.; Clark, G. N. I.; Johnson, M. E.; Head-Gordon, T. *J. Phys. Chem. B* **2010**, *114*, 2549–2564.
(48) Rick, S. W.; Stuart, S. J.; Berne, B. J. *J. Chem. Phys.* **1994**, *101*, 6141–6156.
(49) Bryce, R. A.; Vincent, M. A.; Malcolm, N. O. J.; Hillier, I. H.; Burton, N. A. *J. Chem. Phys.* **1998**, *109*, 3077–3085.
(50) Chen, B.; Xing, J. H.; Siepmann, J. I. *J. Phys. Chem. B* **2000**, *104*, 2391–2401.
(51) Yoshida, N.; Kato, S. *J. Chem. Phys.* **2000**, *113*, 4974–4984.
(52) Mannfors, B.; Palmo, K.; Krimm, S. *J. Mol. Struct.* **2000**, *556*, 1–21.
(53) Llanta, E.; Ando, K.; Rey, R. *J. Phys. Chem. B* **2001**, *105*, 7783–7791.
(54) Banks, J. L.; Kaminski, G. A.; Zhou, R. H.; Mainz, D. T.; Berne, B. J.; Friesner, R. A. *J. Chem. Phys.* **1999**, *110*, 741–754.
(55) Patel, S.; Mackerell, A. D.; Brooks, C. L. *J. Comput. Chem.* **2004**, *25*, 1504–1514.
(56) Patel, S.; Brooks, C. L. *J. Comput. Chem.* **2004**, *25*, 1–15.
(57) Dick, B. G.; Overhauser, A. W. *Phys. Rev.* **1958**, *112*, 90–103.
(58) Stuart, S. J.; Berne, B. J. *J. Phys. Chem.* **1996**, *100*, 11934–11943.
(59) Pratt, L. R. *Mol. Phys.* **1980**, *40*, 347–360.
(60) Lamoureux, G.; Roux, B. *J. Chem. Phys.* **2003**, *119*, 3025–3039.
(61) Lamoureux, G.; MacKerell, A. D.; Roux, B. *J. Chem. Phys.* **2003**, *119*, 5185–5197.
(62) Lindan, P. J. D.; Gillan, M. J. *J. Phys.-Condens. Matter* **1993**, *5*, 1019–1030.
(63) van Maaren, P. J.; van der Spoel, D. *J. Phys. Chem. B* **2001**, *105*, 2618–2626.
(64) Yu, H. B.; Hansson, T.; van Gunsteren, W. F. *J. Chem. Phys.* **2003**, *118*, 221–234.
(65) Yu, H. B.; van Gunsteren, W. F. *J. Chem. Phys.* **2004**, *121*, 9549–9564.
(66) Xie, W. S.; Song, L. C.; Truhlar, D. G.; Gao, J. L. *J. Chem. Phys.* **2008**, *128*, 234108.
(67) Xie, W. S.; Orozco, M.; Truhlar, D. G.; Gao, J. *J. Chem. Theory Comput.* **2009**, *5*, 459–467.

standard particle-based dynamical propagation algorithms. Thus, they can be implemented in existing biomolecular simulation programs without requiring extensive code enhancements.

Our goal here is to develop a Drude oscillator-based polarizable force field able to represent ion−carbonyl interactions with quantitative accuracy. The molecule *N*-methylacetamide (NMA) is chosen to represent the protein peptide linkage. NMA contains a single amide group terminated by methyl groups, making it an excellent surrogate for characterizing the physical properties of the protein backbone. It is widely used in experimental[68,69] as well as computational studies.[31,70−73] In order to construct and optimize the parameters for the force field, the completeness and the quality of the set of "target data" used are of primary importance. System properties that probe ion−NMA interactions, in the bulk phase as well in the gas phase, must be taken into consideration. A very important piece of information is the experimentally determined gas-phase binding enthalpy of NMA with Na^+ and K^+.[68,69] Equally critical are the thermodynamic properties of ion solvation in liquid NMA. Because these latter properties have not, to the best of our knowledge, been characterized in the literature, we have experimentally determined the solubilities and solvation free energies of NaCl and KCl in liquid NMA. In addition to these experimental data, it is advantageous to take results from high-level *ab initio* quantum mechanical methods into consideration. Such "first principles" calculations provide very important information that is not readily available from the experiments. Using this complete set of target data, we develop a new polarizable force field based on the classical Drude oscillator model[60] to represent the interactions of NMA with Na^+, K^+, and Cl^-. The new model is used to identify key features of ion coordination by carbonyl moieties and by water. It also is used to examine the relative free energy of K^+ and Na^+ coordinated in clusters comprising a small number of NMA molecules.

The paper is organized as follows: First, we present the experimental and simulation study details. Then, we summarize the geometric and thermodynamic properties of ion−amide interactions in the gas phase and in the condensed phase. In the end, we present a summary and outlook based on the current work.

Methods

Measurement of Solubilities of NaCl and KCl in Liquid NMA. Crude *N*-methylacetamide (NMA, 99%) was obtained from Alfa Aesar (Pelham, New Hampshire). The NMA was purified by an established fractional freezing method.[74] In detail, NMA was melted in its commercial container by warming to 40 °C in a water bath and poured into a half-jacketed flask similar to the type used by Berger and Dawson,[74] the differences being in design for a circulating system to control the temperature. The NMA (400 mL) was allowed to freeze at 28 °C overnight, and the liquid phase was considered impure following Berger and Dawson.[74] Fractional freezing was repeated three additional times, increasing the freezing temperature each time to ensure that more impurities were removed. A final melting point of 30.2 °C was achieved for the purified NMA, which would indicate a purity of >99.8%.[75] The purified NMA was stored in the half-jacketed flask at room temperature and was kept free of water by means of a stoppered vent with a drying tube containing anhydrous calcium sulfate. NaCl and KCl (Sigma-Aldrich, St. Louis, MO) and pyrex tubes (25 mm ×150 mm, screw top) were oven-dried at 150 °C for at least one week. Water was deionized Milli-Q water. Saturated solutions, at room temperature, were prepared by placing an excess of oven-dried NaCl or KCl (approximately 1−2 g) into an oven-dried tube and adding approximately 10 mL of purified "dry" NMA; in some cases a known amount (4−12%) of water was included. The specific procedures were as follows: defined NMA/water solvent mixtures were prepared by measuring 10.0 mL of purified, dry NMA into an oven-dried 10-mL graduated cylinder and then using a pipet to add 0.41−1.36 mL (4−12%) of water, after which the mixed solvent was added to excess dry NaCl or KCl in an oven-dried tube. Care was taken to ensure that excess salt was present in each experiment. The tubes were flushed briefly with dry N_2 gas and then sealed with Teflon-lined caps.

For experiments at 303.15, 313.15, or 323.15 K, the tubes were initially equilibrated three days in a heating block set at 10 K above the desired final solution temperature (namely at 313.15, 323.15, 333.15 K), to speed the approach to equilibrium. Solutions were mixed by vortexing intermittently during the 3-day period. After the third day, the block temperature was set to the final desired temperature for the remainder of a two-week equilibration period. After two weeks, three aliquots of varying sizes (0.3−0.7 mL) containing only salt solution (no crystals) were removed from each tube using a micropipet and put into preweighed 1.5-mL microfuge tubes. Once the aliquots were removed, the stock solution tube was once again flushed with N_2 gas and was further incubated and saved for future replicate samples. The solvent was removed from the microfuge tubes by vacuum centrifugation, and the tubes were dried under vacuum (10^{-2} mmHg) to constant weight (48−72 h). Dissolved salt concentrations were then determined on the basis of the weight gain of the microfuge tubes. All measurements were made in triplicate on a given day and were repeated on multiple days at 1−2 week intervals.

Potential Energy Functions and Condensed Phase Simulations. To account for induced polarization, a Drude particle carrying a negative charge is bound to an atom via a harmonic spring.[35,60,76] The atom−Drude spring constant K_D is set to 1000 kcal/mol/Å^2 for all Drude oscillators in the system. This value dictates the magnitude of the charge that the Drude particle must carry to produce the correct polarizability α, i.e., $q_D = \sqrt{\alpha K_D}$.[60,76] The methodology on the Drude polarizable models has been documented elsewhere.[35,60] Within this framework, we have developed polarizable models for water,[61,77] aromatic compounds,[78] alcohols,[79] amides,[73] and ions.[34,80,81] Briefly, the simple water model with four-site and negative Drude polarizability (SWM4-NDP) reproduces most properties of bulk water under ambient conditions.[77] The polarizable model of NMA accurately reproduces the anomalously high dielectric constant,[73] a property that usually is poorly described using the nonpolarizable force fields.[82] The ion models were developed and tested for hydration properties.[34,80,81] For comparison, all the calculations were also

(68) Klassen, J. S.; Anderson, S. G.; Blades, A. T.; Kebarle, P. *J. Phys. Chem.* **1996**, *100*, 14218–14227.
(69) Tsang, Y.; Siu, F. M.; Ho, S. S.; Ma, N. L.; Tsang, C. W. *Rapid Commun. Mass Spectrom.* **2004**, *18*, 345–355.
(70) Whitfield, T. W.; Martyna, G. J.; Allison, S.; Bates, S. P.; Crain, J. *Chem. Phys. Lett.* **2005**, *414*, 210–214.
(71) Whitfield, T. W.; Crain, J.; Martyna, G. J. *J. Chem. Phys.* **2006**, *124*, 094503.
(72) Li, Z. Y.; Yu, H. B.; Zhuang, W.; Mukamel, S. *Chem. Phys. Lett.* **2008**, *452*, 78–83.
(73) Harder, E.; Anisimov, V. M.; Whitfield, T.; MacKerell Jr, A. D.; Roux, B. *J. Phys. Chem. B* **2008**, *112*, 3509–3521.
(74) Berger, C.; Dawson, L. R. *Anal. Chem.* **1952**, *24*, 994–996.
(75) Dawson, L. R.; Eckstrom, H. C.; Sheridan, R. C. *J. Phys. Chem.* **1961**, *65*, 1829–1831.
(76) Drude, P. *Lehrbuch der Optik*; S. Hirzel: Leipzig, 1900. English translation: *The Theory of Optics*; Drude, P., translated from the German by C. Riborg Mann and Robert A. Mill; Longmans, Green and Co.: New York, 1907.
(77) Lamoureux, G.; Harder, E.; Vorobyov, I. V.; Roux, B.; MacKerell, A. D. *Chem. Phys. Lett.* **2006**, *418*, 245–249.
(78) Lopes, P. E. M.; Lamoureux, G.; Roux, B.; MacKerell, A. D. *J. Phys. Chem. B* **2007**, *111*, 2873–2885.

carried out using the nonpolarizable additive CHARMM force field PARAM27,[9] with the TIP3P water model,[20] and the ion models with the optimized Lennard-Jones parameters.[83,84]

The condensed phase simulations were performed using the program CHARMM[85] (version c35a1). The system, including an ion at the center of a cubic box with 144 NMA molecules or 216 water molecules, was simulated under periodic boundary conditions (PBC) at constant temperature and constant pressure of 1 atm using a modified Andersen−Hoover barostat.[86] Temperature in the system was controlled via two Nosé−Hoover (NH) thermostats.[87,88] To mimic the self-consistent field (SCF) condition while retaining computational efficiency, the Drude oscillators were simulated using an extended Lagrangian in which the reduced mass within the local atom−Drude reference frame was coupled to a NH thermostat at 1 K.[60] A second NH thermostat coupled to the center of mass of the atom−Drude pair maintained the temperature of the bulk at 303.15 K. A particle mesh approximation to the Ewald sum (PME) was used with "tin foil" boundary conditions to evaluate the Coulombic interactions in the liquid simulations.[89] The bonds involving hydrogen atoms were constrained using the SHAKE algorithm,[90] and the time step was set to 1 fs.

Free Energy Simulations. The solvation free energy of the ions ΔG_{solv} was computed according to a step-by-step reversible work procedure during which the ion−solvent core repulsion (rep), the ion−solvent van der Waals dispersive attraction (dis), and the ion−solvent electrostatic (elec) interactions were switched on sequentially.[91] ΔG_{solv} is obtained as the sum $\Delta G_{rep} + \Delta G_{dis} + \Delta G_{elec}$. Each contribution to the total hydration free energy was computed from independent simulations. The repulsive contribution, ΔG_{rep}, was computed using a soft-core scheme to avoid the end-point singularity in free energy calculations[91,92] and was unbiased using the weighted histogram analysis method (WHAM).[93−96] The electrostatic and dispersive contributions ΔG_{elec} and ΔG_{dis} were computed using thermodynamic integration (TI). The computational protocol is documented in ref 81. A similar series of calculations was carried out at 323.15 K to obtain the enthalpy and entropy components of the solvation free energy. Additional calculations with 512 water molecules showed little variation in the contributions to the charging solvation free energy ΔG_{elec} of K^+ (less than 0.3 kcal/mol), indicating that finite-sized artifacts are small in the current setup.[81]

In discussions of the solvation free energy of ionic species, one may either consider the *real* physical value, which includes the contribution of the phase potential arising from crossing the physical air−liquid interface, or the *intrinsic* bulk phase value, which is independent of the interfacial potential.[80,97−100] Throughout the present study, only *real* solvation free energies are reported in order to avoid any ambiguity in the absolute thermodynamic scale. The latter corresponds to the reversible thermodynamic work to move a single ion from vacuum to the interior of a pure liquid phase (i.e., across the physical liquid−vacuum interface). See the discussions in refs 80, and 81 and references therein. For ions carrying a charge z, the *real* and *intrinsic* solvation free energies differ by an offset constant, $\Delta G^{real} = \Delta G^{intr} + zF\Phi$, where F is the Faraday constant (23.06 kcal/mol/V) and Φ is the phase potential of the liquid relative to vacuum. The contribution from Φ cancels out when considering the cation−anion neutral pair but is present for charged species. Because the solvation free energy calculations with PBC and PME are carried out within a particle-sum (P-sum) convention,[97,98] the reference phase potential of the bulk liquid is the internal Galvani potential. Implicitly, such free energy calculations yield ΔG^{intr} by definition. To obtain the physically meaningful ΔG^{real}, this value needs to be shifted by $zF\Phi$, where Φ must be calculated via the same P-sum convention. For the water−vacuum interface, the phase potential calculated via a P-sum internal Galvani potential with the SWM4-NDP water model is about −545 mV.[77] The interfacial potential Φ of the NMA−vacuum interface was calculated for PARAM27 and the Drude polarizable model using the same method. The simulation systems represent a slab of 144 NMA molecules, periodic in XY and presenting two NMA−vacuum interfaces along the Z axis. The charge density along the Z axis was averaged from 10 ns simulations carried out at 303 K, and the potential profile $\Phi(z)$ across the entire system was calculated by numerically integrating the one-dimensional Poisson equation. Values of −344 mV and −194 mV were obtained for PARAM27 and the Drude polarizable model, respectively. Asymmetric deviations of the potential profile between the two sides of the central NMA slab (i.e., comparing $\Phi(z = 0)$ and $\Phi(Z = L)$) indicate that the values are statistically converged within about 6 mV.

The relative free energy of K^+ and Na^+ coordinated in small clusters comprising 1 to 8 NMA or water molecules was calculated using the Drude polarizable models. For comparison, the relative free energy was also calculating using the nonpolarizable models.[9,20,84] As in previous studies,[84,101,102] the oxygen atoms of the clusters were constrained to remain confined within a spherical region of 3.5 Å radius by a flat-bottom half-harmonic potential with a force constant of 100 kcal/mol/Å^2 but were otherwise unrestrained. Selectivity of a binding site model is governed by the relative free energy of ion i and j, $\Delta\Delta G_{ij} = \Delta G_{ij}^{site} - \Delta G_{ij}^{water}$, where $\Delta G_{ij}^{water} = [G_i^{water} - G_j^{water}]$ is the difference in hydration free energy between ion i and j, and $\Delta G_{ij}^{site} = [G_i^{site} - G_j^{site}]$ is the free energy difference between ion i and j in the binding site. The relative hydration free energy ΔG_{ij}^{water} was taken from previous work.[81] The relative free energies ΔG_{ij}^{site} were calculated using free energy perturbation/MD simulations, generated for a total sampling time of 2 ns, and postprocessed using WHAM.[93−96]

Parameterization Strategy. The general strategy for parametrizing the polarizable force field has been documented elsewhere.[34,60,61,73,77−80,103,104] Here we briefly summarize the technical details for optimizing the Lennard-Jones (LJ) parameters

(79) Anisimov, V. M.; Vorobyov, I. V.; Roux, B.; MacKerell, A. D. *J. Chem. Theory Comput.* **2007**, *3*, 1927–1946.
(80) Lamoureux, G.; Roux, B. *J. Phys. Chem. B* **2006**, *110*, 3308–3322.
(81) Yu, H. B.; Whitfield, T. W.; Harder, E.; Lamoureux, G.; Anisimov, V. M.; MacKerell, A. D. J.; Roux, B. *J. Chem. Theory Comput.* **2010**, *6*, 774–786.
(82) Whitfield, T.; Martyna, G.; Allison, S.; Bates, S.; Vass, H.; Crain, J. *J. Phys. Chem. B* **2006**, *110*, 3624–3637.
(83) Beglov, D.; Roux, B. *J. Chem. Phys.* **1994**, *100*, 9050–9063.
(84) Noskov, S. Y.; Berneche, S.; Roux, B. *Nature* **2004**, *431*, 830–834.
(85) Brooks, B. R.; et al. *J. Comput. Chem.* **2009**, *30*, 1545–1614.
(86) Martyna, G.; Tobias, D.; Klein, M. *J. Chem. Phys.* **1994**, *101*, 4177–4189.
(87) Nosé, S. *J. Chem. Phys.* **1984**, *81*, 511–519.
(88) Hoover, W. *Phys. Rev. A* **1985**, *31*, 1695–1697.
(89) Essmann, U.; Perera, L.; Berkowitz, M. L.; Darden, T.; Lee, H.; Pedersen, L. G. *J. Chem. Phys.* **1995**, *103*, 8577–8593.
(90) Ryckaert, J. P.; Ciccotti, G.; Berendsen, H. J. C. *J. Comput. Phys.* **1977**, *23*, 327–341.
(91) Deng, Y.; Roux, B. *J. Phys. Chem. B* **2004**, *108*, 16567–16576.
(92) Beutler, T. C.; Mark, A. E.; van Schaik, R. C.; Gerber, P. R.; van Gunsteren, W. F. *Chem. Phys. Lett.* **1994**, *222*, 529–539.
(93) Kumar, S.; Bouzida, D.; Swendsen, R. H.; Kollman, P. A.; Rosenberg, J. M. *J. Comput. Chem.* **1992**, *13*, 1011–1021.
(94) Kumar, S.; Rosenberg, J. M.; Bouzida, D.; Swendsen, R. H.; Kollman, P. A. *J. Comput. Chem.* **1995**, *16*, 1339–1350.
(95) Roux, B. *Comput. Phys. Commun.* **1995**, *91*, 275–282.
(96) Souaille, M.; Roux, B. *Comput. Phys. Commun.* **2001**, *135*, 40–57.
(97) Kastenholz, M.; Hunenberger, P. *J. Chem. Phys.* **2006**, *124*, 124106.
(98) Kastenholz, M. A.; Huenenberger, P. H. *J. Chem. Phys.* **2006**, *124*, 224501.
(99) Asthagiri, D.; Pratt, L. R.; Ashbaugh, H. S. *J. Chem. Phys.* **2003**, *119*, 2702–2708.
(100) Harder, E.; Roux, B. *J. Chem. Phys.* **2008**, *129*, 234706.
(101) Noskov, S. Y.; Roux, B. *J. Gen. Physiol.* **2007**, *129*, 135–143.
(102) Yu, H. B.; Noskov, S. Y.; Roux, B. *J. Phys. Chem. B* **2009**, *113*, 8725–8730.
(103) Anisimov, V. M.; Lamoureux, G.; Vorobyov, I. V.; Huang, N.; Roux, B.; MacKerell, A. D. *J. Chem. Theory Comput.* **2005**, *1*, 153–168.
(104) Harder, E.; Anisimov, V. M.; Vorobyov, I. V.; Lopes, P. E. M.; Noskov, S. Y.; MacKerell, A. D.; Roux, B. *J. Chem. Theory. Comput.* **2006**, *2*, 1587–1597.

between ions (in our case Na^+, K^+, and Cl^-) and the carbonyl oxygen atom or the amide nitrogen atom in amides. By default, the parameters of the LJ 6−12 interaction E^{ij}_{min} and R^{ij}_{min} for the *ij* atom pair are generated using the Lorentz−Berthelot combination rule: $E^{ij}_{min} = (E^{ii}_{min}E^{jj}_{min})^{1/2}$ and $R^{ij}_{min} = (R^{ii}_{min} + R^{jj}_{min})/2$. To have more freedom to optimize the ion−NMA interactions, it is possible to override the default values from the combination rule and assign a set of specific pairwise LJ parameters via the "NBFIX" option of the CHARMM parameter file.[85,105] The target values are the gas-phase ion−NMA interactions (including binding energies and geometric properties) and the solvation free energy in liquid NMA.

Due to the uncertainties about the absolute solvation free energy of single ions, we focus on the total solvation free energy of the neutral salts and the relative solvation free energy between Na^+ and K^+, as was done as in previous work.[31,34,80,81] The standard states for the experimental transfer free energy from the gas phase to the liquid phase are typically chosen to be a gas at 1 atm and a 1 molar solution. Consequently, a correction of 1.9 kcal/mol is added to the calculated solvation free energy of a single ion and 3.8 kcal/mol is added to that of a whole salt when comparing the simulations against the experimentally derived solvation free energies.[31,34,80]

During the optimization of the LJ parameters, the well depth of the van der Waals dispersive interactions between a specific atom pair was kept constant, and equal to the default well depth, using the standard Lorentz−Berthelot combination rule in the CHARMM force field.[9] In practice, a series of pair-specific LJ parameters (NBFIX) for the van der Waals radii were generated based the ion−NMA interactions in the gas phase. Generally, a grid based search was performed by varying R^{ij}_{min} between 4% above and below the default value. Then, a number of candidates were chosen to further characterize the ion solvation free energy in liquid NMA. In practice, we first focused on the models for K^+ and Cl^- and achieved the Na^+ model by FEP based on the K^+ to take advantage of the better convergence of the relative solvation free energy calculations. Based on both the gas phase dimer properties and the solvation free energies in liquid NMA, a final model was chosen (See Supporting Materials for the parameters). The optimized R^{ij}_{min} values deviate from the default values (i.e., the Lorentz−Berthelot combination rules) by less than 2%.

Ab Initio Simulations. All electron *ab initio* calculations were performed for the ion−NMA dimers in the gas phase using the Gaussian 03[106] package at the MP2 level with the 6-311++G(2df,2pd) basis set. The basis set superposition errors (BSSE) were taken into account using the Boys−Bernadi counterpoise correction.[107]

First-principles MD simulations were carried out based on density functional theory (DFT) within the Car−Parrinello MD scheme[108] using the PINY_MD[109,110] and CPMD[111] software packages. The simulation system includes 16 NMA molecules and one cation (K^+ or Na^+) in a cubic box of length 12.6 Å simulated with PBC. The initial configurations were taken from well-equilibrated Drude polarizable systems. As the polarizable model reproduces the *ab initio* coordination structure (see below), it is expected that extensive equilibration is not required.

A DFT/MD simulation of K^+ in NMA was carried out with PINY_MD.[109,110] The simulation was based on the BLYP exchange-correlation functional[112,113] with a plane-wave basis set (BLYP/pw) and a 70 Ry cutoff. Martins-Troullier norm-conserving pseudopotentials[114] were used throughout and the semicore (3*s* and 3*p*) states were included in the valence electrons for K^+. A baseline fictitious electronic mass of 475 au was used with mass preconditioning.[115] The canonical ensemble was sampled with MD propagated with a time-step of 0.125 fs, and adiabaticity between the nuclear and electronic degrees of freedom was maintained with NH chains.[87,88,116−120] After an initial wave function minimization and 0.5 ps of equilibration, data were collected over 24 ps of production. The temperature over the course of the DFT/MD simulation was 297 ± 15 K.

A DFT/MD simulation of Na^+ in NMA was carried out using CPMD.[111] The BLYP exchange-correlation functional[112,113] with a plane-wave basis set (BLYP/pw) and a cutoff of 80 Ry were used with the norm-conserving Goedecker pseudopotential (including the semicore 2*s* and 2*p* states for Na^+).[115] The canonical ensemble was sampled with MD propagated with a time-step of 4 au (~0.1 fs) and a fictitious mass of 400 au for the electrons, and adiabaticity between the nuclear and electronic degrees of freedom was maintained with two NH thermostats[87,88] After an initial wave function minimization and 0.5 ps of equilibration, data were collected over 20 ps of production. The temperature over the course of the simulation was 303 ± 16 K.

The influence of the sampling time and of the finite size of the simulation systems on the radial distribution function (RDF) and the coordination number of Na^+ and K^+ in liquid NMA were examined using simulations based on the Drude models, used as a "surrogate" for the DFT representation (see Supporting Materials). Finite-size effects on the RDFs and the coordination numbers were assessed by comparing the results with 16, 32, or 144 NMA based on the Drude polarizable force field, and were found to be very small. Furthermore, the convergence of the RDF and the coordination number was probed by comparing multiple 20 ps simulations based on the Drude models, starting from randomly chosen snapshots taken from the nonpolarizable models. The statistical analyses on the RDFs calculated from the relatively short DFT/MD simulations were determined by dividing the total trajectory into 2 ps parts and calculating the error in the mean of each histogram window.[34] All these results indicate that the RDF and the coordination numbers from the DFT/MD simulations are statistically meaningful and that there are no important finite-size effects.

Results and Discussion

Experimental Determination of NaCl and KCl Solubilities in Liquid NMA. Solubilities were measured for KCl and NaCl in purified, dry NMA. Both salts are modestly soluble in liquid NMA. Repeated sampling at one-week intervals indicated small increases in the dissolved salt concentrations for all samples over a 2−4 week interval, at which time the measurements leveled, indicating that saturation was achieved. The results at

(105) Baker, C. M.; Lopes, P. E. M.; Zhu, X.; Roux, B.; MacKerell, A. D. *J. Chem. Theory Comput.* **2010**, *6*, 1181–1198.
(106) Frisch, M. J.; et al. *Gaussian 03*, Revision C.02; Gaussian, Inc.: Wallingford, CT, 2004.
(107) Boys, S. F.; Bernardi, F. *Mol. Phys.* **1970**, *19*, 553–566.
(108) Car, R.; Parrinello, M. *Phys. Rev. Lett.* **1985**, *55*, 2471–2474.
(109) Samuelson, S.; Martyna, G. *J. Chem. Phys.* **1998**, *109*, 11061–11073.
(110) Tuckerman, M. E.; Yarne, D.; Samuelson, S. O.; Hughes, A. L.; Martyna, G. J. *Comput. Phys. Commun.* **2000**, *128*, 333–376.
(111) *CPMD*, Car−Parrinello Molecular Dynamics: An ab Initio Electronic Structure and Molecular Dynamics Program; CPMD Consortium, IBM Corp. and MPI fr Festkrperforschung, Stuttgart; http://www.cpmd.org.
(112) Becke, A. D. *Phys. Rev. A* **1988**, *38*, 3098–3100.
(113) Lee, C.; Yang, W.; Parr, R. G. *Phys. Rev. B* **1988**, *37*, 785–789.
(114) Troullier, N.; Martins, J. L. *Phys. Rev. B* **1991**, *43*, 1993–2006.
(115) Tassone, F.; Mauri, F.; Car, R. *Phys. Rev. B* **1994**, *50*, 10561–10573.
(116) Martyna, G. J.; Klein, M. L.; Tuckerman, M. *J. Chem. Phys.* **1992**, *97*, 2635–2643.
(117) Tuckerman, M. E.; Parrinello, M. *J. Chem. Phys.* **1994**, *101*, 1302–1315.
(118) Tuckerman, M. E.; Parrinello, M. *J. Chem. Phys.* **1994**, *101*, 1316–1329.
(119) Hutter, J.; Tuckerman, M. E.; Parrinello, M. *J. Chem. Phys.* **1995**, *102*, 859–871.
(120) Martyna, G. J.; Tuckerman, M. E.; Tobias, D. J.; Klein, M. L. *Mol. Phys.* **1996**, *87*, 1117–1157.
(121) Goedecker, S.; Teter, M.; Hutter, J. *Phys. Rev. B* **1996**, *54*, 1703–1710.
(122) Marcus, Y. *Ion Solvation*, 1st ed.; John Wiley & Sons: New York, 1985.

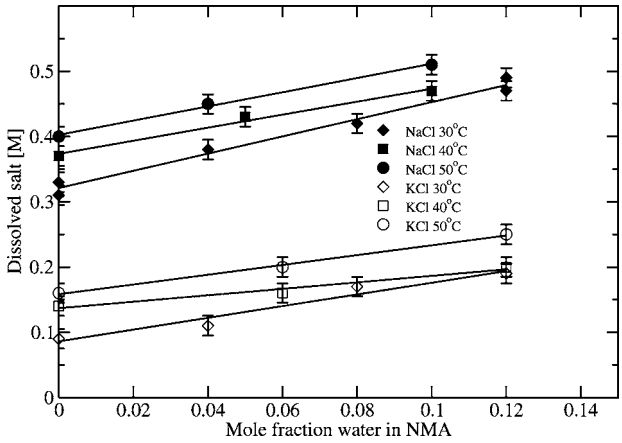

Figure 1. Solubility of NaCl (filled symbols) or KCl (open symbols) as function of the mole fraction of water in liquid NMA.

Table 1. Solubilities of NaCl and KCl in Water, Dry Formamide and Dry NMA Measured at Different Temperatures

		saturating concentration (mol/L)		
salts	temp (K)	water[a]	formamide[b]	NMA[c]
NaCl	303.15	5.44	0.89	0.32
	313.15	5.48	–	0.37
	323.15	5.52	–	0.40
KCl	303.15	4.29	1.67	0.09
	313.15	4.57	–	0.13
	323.15	4.85	–	0.16

[a] The listed solubilities in water are derived based on the values obtained from *CRC Handbook of Chemistry and Physics*.[124] [b] The listed solubilities in formamide is taken from ref 125 measured at 298.15 K. [c] The listed solubilities in NMA are the intercepts of the linear fits to the data in Figure 1. Based upon repeated measurements (at least 2 sets of 3 repetitions), the estimated uncertainty in the intercept is 0.012 M.

each temperature, averaged from six to nine samples at saturation, are shown in Figure 1 and Table 1. As a check on the method, small known amounts of water were added to some of the NMA samples. The linear dependence of each salt solubility on the percentage of water that is mixed with the NMA (Figure 1) lends confidence to the results obtained using purified, "water-free" NMA.

The results show a linear increase of the salt concentration with the addition of water to NMA. The solubility also increases with increasing temperature. Although the increases are small, the trends appear to be uniform over the 20 °C temperature range. These results yield information about the solubilities in dry NMA because the addition of small amounts of water linearly increases the solubility, making it possible to extrapolate to a zero point with the same value as the tested zero point. Though we estimate, from the freezing point, the water content of the purified NMA to be <0.1%, the numbers in Table 1 should nevertheless be considered upper limits. In spite of the precautions taken, we cannot exclude the possibility that inadvertent traces of water *could* remain with the purified NMA. Such water, if present, would increase the solubilities of NaCl and KCl, such that the actual solubilities of KCl and NaCl in liquid NMA alone could be slightly lower than the values listed in Table 1.

(123) Cox, B. G.; Hedwig, G. R.; Parker, A. J.; Watts, D. W. *Aust. J. Chem.* **1974**, *27*, 477–501.
(124) Lide, D. R., Ed. *CRC Handbook of Chemistry and Physics*; CRC Press Taylor & Francis Group: Boca Raton, FL, 2008.
(125) Burgess, J. *Ions in Solution: Basic Principles of Chemical Interactions*, 2nd ed.; Horwood Publishing: New York, 1999.

Table 2. Experimentally Derived Solvation Free Energies (kcal/mol)

	water[126]	formamide[a]	NMA[b]
KCl	−156.5	−154.4	−153.0
	(−17.5)	(−18.2)	(−18.1)
NaCl	−174.0	−172.6	−171.6

[a] The solvation free energies in formamide are derived by combining the water solvation data from Schmid et al.[126] with the transfer free energies from Cox et al.[123] [b] The estimates for the solvation free energies for NaCl and KCl in NMA are derived from the solvation free energies in formamide [123,126] and the transfer free energies between formamide and NMA.

Solvation Free Energies of Salts in Liquid NMA. The transfer free energy of a salt going from a saturated solution (molarity χ_A) in solvent A to a saturated solution (molarity χ_B) in B can be deduced by considering the two thermodynamic equilibria between the saturated solution (with solvent A or with solvent B) and the crystalline state of the salt at temperature *T*. The basis for relating the solvation free energies is that the chemical potential of the ions in the undissolved salt crystal is the same, whether it is in solvent A or B. Thus, the transfer solvation free energy for going from solvent A to solvent B at temperature *T* can be calculated by the following equation

$$\Delta\Delta G_{A\to B} = -k_B T \ln\left[\frac{\gamma_B \chi_B}{\gamma_A \chi_A}\right] \quad (1)$$

where γ_A and γ_B are the activity coefficients of the salt at the molarities χ_A or χ_B in solvent A or B, respectively. A few caveats associated with the application of eq 1 should be noted. Equation 1 is concerned with the solvation free energy difference of the salt at finite concentration in solvent A or B, which in this case are the saturated concentrations. Activity coefficients of salt (γ) in various nonaqueous solvents are usually not available.[122] In extracting solvation free energies from eq 1, it must be assumed either that both solutions are ideal (with $\gamma = 1$), or that the activity coefficients are very similar at the saturated concentration in the two solvents. Furthermore, the experiments for different solvents might be performed at slightly different temperatures (usually around room temperature), which also introduces some uncertainty in the calculated solvation free energies. To minimize the error caused by possible differences in activity coefficients, we choose formamide as a reference, in view of the similar solubilities of the salts in formamide and NMA. This is a reasonable expectation because the activity coefficient of a salt reflects the indirect effect of ion−ion solvent-shielded interactions on the solvation free energy of ions. The solvation free energies of the NaCl and KCl salts in liquid NMA relative to formamide are estimated to be 1.36 and 0.98 kcal/mol, respectively. The total solvation free energies of the salts are given in Table 2. The error introduced by using eq 1 is estimated to be about 1 kcal/mol, obtained by comparing the transfer free energies from water to formamide for NaCl and KCl with the available experimental data obtained by Cox et al.[123−125] Using water as a reference with eq 1 might yield slightly different and less accurate values due to the large difference in salt solubilities compared to NMA. The solvation free energies of the whole salts in different solvents are within ~2 kcal/mol of one another. The solvation free energy difference

Table 3. Ion−NMA Complex in the Gas Phase[a]

	K^+			Na^+			Cl^-		
system and model	ΔE	$R(K^+-O)$	ΔH^b	ΔE	$R(Na^+-O)$	ΔH^b	ΔE	$R(Cl^-H)$	ΔH^b
PARAM27	−24.2	2.54	−23.9	−31.1	2.15	−30.9	−17.4	2.20	−17.1
PARAM27/NBFIX	−22.1	2.68	−21.8	−27.3	2.34	−27.1	−17.4	2.20	−17.1
AMOEBA[31]	−27.7	2.46		−36.4	2.10	−	−23.4	2.25	
Drude	−29.8	2.57	−29.2	−41.5	2.19	−41.0	−24.5	2.11	−24.2
ab initio[69,31]		2.43	−30.3		2.10	−38.1			
ab initio[c]	−30.9	2.47		−38.7	2.15		−23.9	2.08	
ab initio[d]	−28.6	2.46		−36.9	2.18				
CID exp[68]			−30.4			−35.7			

[a] ΔE (in kcal/mol) is the energy minimum, and R (in Å) is the ion−atom(NMA) distance in the optimized complex. [b] The binding enthalpies ΔH (in kcal/mol) are calculated at 298.15 K. [c] MP2/6-311++G(2df,2pd) with BSSE correction. [d] Calculations based on the same model as used in first-principles DFT/MD simulations of K^+ and Na^+.

between K^+ and Na^+ in formamide and in NMA is around 18 kcal/mol, which is similar to that in water.[126]

Ion−Amide Complexes in the Gas Phase. All available information about the interaction of K^+ and Na^+ with NMA is summarized in Table 3. Some of the most valuable data about the microscopic interactions are provided by gas phase experiments and *ab initio* studies. The classic gas-phase measurements by Kebarle and co-workers have provided fundamental information about ion hydration and the microscopic interactions in small clusters[127,128] The data about the interactions of cations with amides are less extensive. The binding energies of K^+ to dimethylacetamide and to dimethylformamide have been measured using mass spectroscopy.[68] There are also estimates of Li^+ affinity for dimethylformamide[129] and for formaldehyde[130] from cyclotron resonance spectroscopy. Klassen et al. have used collision-induced-dissociation (CID) threshold data to experimentally derive the binding enthalpies of K^+ and Na^+ to acetamide, NMA, *N*,*N*-dimethylacetamide, glycine, and diglycine.[68]

High level *ab initio* calculations on similar model systems play an important role to complement and strengthen our confidence in the gas-phase experimental data. In this regard, the extensive study of alkali metal and amide dimers performed by Siu et al.[69,131] provide an important source of information. The measured binding enthalpies of K^+ and Na^+ with NMA are −30.4 and −35.7 kcal/mol, respectively, with an estimated error of 3.0 kcal/mol.[68] The calculated binding energies of K^+ and Na^+ with NMA are −30.3 and −38.1 kcal/mol, respectively.[69,131] The results compare well with the present *ab initio* calculations at the MP2/6-311++G(2df,2pd) level, yielding ion−NMA binding energies of −30.9 and −38.7 kcal/mol for K^+ and Na^+, respectively. The distance between the carbonyl oxygen and the cation in the optimized ion−NMA complex is 2.15 and 2.47 Å for Na^+ and K^+, respectively. It is worth noting that the interactions of cations with NMA is larger by about 50 to 60% compared to water; for example, the binding energy of K^+ with a water molecule is −17.9 kcal/mol[127,128] and is −30.4 kcal/mol with NMA.[68]

Both nonpolarizable force fields give less favorable binding energies and longer distances for both the cations and the anion.[18,101] In the default PARAM27 model, the LJ parameter of the ion, which was optimized to reproduce the hydration free energy, is simply extended to the ion−carbonyl oxygen pair interaction via the standard combination rule.[83] In the second model, PARAM27/NBFIX, a choice was made to adjust the LJ parameters for the ion−carbonyl oxygen pair in order to match the solvation free energy of an ion in liquid NMA to the hydration free energy.[84] The limitations of those nonpolarizable force fields have been noted previously,[18] and are due to the adopted parametrization protocol aiming to yield reasonable solvational properties, which is achieved at the expense of the gas-phase properties.[18,101] In contrast, the Drude models greatly improve the description of the ion−NMA interactions in terms of binding energies and the cation−oxygen distances. The results obtained from the Drude models are in good agreement with both the experimentally and theoretically gas-phase-derived values.

Table 4. Ions Solvation Free Energy in Liquid NMA (kcal/mol)

models	K^+	Na^+	K^+/Na^+	Cl^-	KCl	NaCl
PARAM27	−86.2	−104.1	(−17.9)	−61.4	−147.6	−165.5
PARAM27/NBFIX	−79.3	−95.6	(−16.0)	−61.4	−140.7	−157.0
Drude	−88.7	−106.7	(−18.0)	−64.9	−153.6	−171.6
Exp.(Table 2)	−	−	(−18.6)	−	−153.0	−171.6

Solvation Free Energy of Ions in Liquid NMA. The solvation free energies of single ions and neutral salts in liquid NMA are listed in Table 4. The nonpolarizable force fields PARAM27 and PARAM27/NBFIX underestimate the solvation free energy for both salts in liquid NMA, sometimes by as much as ∼15 kcal/mol. This is consistent with the underestimated ion−NMA interactions displayed in Table 3. In contrast, the polarizable Drude model succeeds in matching the experimental results very well, with deviations of ∼0.6 kcal/mol for both salts in NMA. The error is smaller than the uncertainty in the derivation of the experimental data.

The solvent−solvent transfer free energies of the salts from water to NMA are reproduced very well for both NaCl and KCl, with a deviation about 0.5 kcal/mol. The transfer of NaCl from water to NMA is 2.7 kcal/mol from the Drude polarizable model, close to the value of 2.4 kcal/mol estimated from experiments; the corresponding results for KCl are 3.6 and 3.5 kcal/mol. Unsurprisingly, the results from the nonpolarizable model are much worse, about 7−8 kcal/mol for the default PARAM27 model and about 14−16 kcal/mol with the PARAM27/NBFIX model. This analysis indicates that the default PARAM27 model, despite the large error, is actually more representative of the correct values than PARAM27/NBFIX.

While the models were directly optimized to reproduce the total solvation free energy of the neutral salts, ΔG, the relative

(126) Schmid, R.; Miah, A. M.; Sapunov, V. N. *Phys. Chem. Chem. Phys.* **2000**, *2*, 97–102.
(127) Diźdić, I.; Kebarle, P. *J. Phys. Chem.* **1970**, *74*, 1466–1474.
(128) Peschke, M.; Blades, A. T.; Kebarle, P. *J. Am. Chem. Soc.* **2000**, *122*, 10440–10449.
(129) Stanley, R.; Beauchamp, J. *J. Am. Chem. Soc.* **1975**, *97*, 5920–5921.
(130) Woodin, R.; Beauchamp, J. *J. Am. Chem. Soc.* **1978**, *100*, 501–508.
(131) Siu, F. M.; Ma, N. L.; Tsang, C. W. *J. Chem. Phys.* **2001**, *114*, 7045–7051.

magnitude of the enthalpic and entropic contributions, $\Delta H - T\Delta S$, is not included in the parametrization procedure.[132] To ascertain how well the Drude polarizable force field is able to capture correctly the balance of enthalpy and entropy, we calculated the temperature-dependent solvation free energies of the salts in water and in liquid NMA. To obtain experimental estimate for the salts in NMA, it is necessary to make use of additional experimental measurements for the solvation of the salts at a different temperature in water and formamide[123,126] (essentially using NMA as solvent A and water as solvent B in eq 1). The experimental estimates of $-T\Delta S$ for KCl and NaCl in NMA are 6 and 11 kcal/mol, respectively. For the Drude polarizable model, the entropy was obtained by finite difference from the solvation free energy of the ions in NMA calculated at two different temperatures, 303.15 and 323.15 K. The computed estimates of $-T\Delta S$ for KCl and NaCl in NMA are 22 and 28 kcal/mol, respectively. For comparison, the experimental values of $-T\Delta S$ for KCl and NaCl in water are 9 and 11 kcal/mol, respectively, while the corresponding values from the Drude polarizable model are 16 and 13 kcal/mol. It is important to realize that there is a considerable uncertainty on the computational estimates due to the imperfect convergence of the free energy simulations. It is at least on the order of about 10 kcal/mol, assuming a minimal error on the order of 0.5 kcal/mol on the solvation free energies. While the calculated entropic components have roughly the correct order of magnitude, there appears to be a general tendency to slightly overestimate this component. The corollary is that the enthalpic component is slightly too negative, e.g., for KCl in NMA, the free energy is −157.2 kcal/mol, the enthalpy is −179 kcal/mol, and the entropy ($-T\Delta S$) is 22 kcal/mol. The origin of such a trend could be due to the utilization of the LJ potential, which gives rise to a harsher core repulsion than the relatively softer repulsion observed in *ab initio* calculations. Nevertheless, there is generally a good accord between the calculated and the experimentally derived numbers, which gives additional confidence that the present polarizable models properly describe both the enthalpic and entropic contributions to the energetic interactions between ions and water/amides.

While the experiments serve to accurately measure the thermodynamic results for the neutral salts, the single ion solvation free energies cannot be determined without additional assumptions. These issues are related to the fact that there is no thermodynamic system where one can actually measure the solvation free energy of charged species without ambiguities. The solvated free energy of the single ions can only be determined within an additive valence-dependent offset constant due to the undetermined phase and interfacial potentials. The present computational models, in which the thermodynamics of the neutral salts (Table 4) is enforced together with the ion−NMA gas-phase interactions (Table 3), offer one possible route to gain information about this important property that is experimentally inaccessible. According to the polarizable Drude models, the absolute solvation free energies of K^+, Na^+, and Cl^- in liquid NMA are −88.7, −106.7, and −64.9 kcal/mol (*real* values). In comparison, the solvation free energies of these ions in water are −78.6, −96.3, and −78.4 kcal/mol, respectively.[81] This analysis leads to the somewhat unexpected observation that liquid NMA is actually a better solvent for cations than liquid water. It is interesting to note that the narrow pores of the KcsA and gA channels are lined by backbone carbonyl groups to coordinate the permeating ion. Although the specific arrangement of the carbonyl groups differ between the two channels, these two cation-selective channels are absolutely impermeable to anions.[84,102,133] Superficially, the very favorable solvation free energy of the cations in NMA may appear inconsistent with the relatively low solubility of the neutral salts. However, it is important to keep in mind that NMA does not solvate Cl^- as well as water. The present results would predict that the solubility of a neutral salt comprising K^+ or Na^+ paired with a large hydrophobic anion could be considerably larger in NMA than in water. Interestingly, salts involving the large anion tetraphenylborate ($TBPh_4$), such as $NaTBPh_4$ and $KTBPh_4$, are typically more soluble in organic solvent than in water. Notably, the solubility of $KTBPh_4$ is very low in water, but is much higher in acetone and other organic solvents.[134] The very favorable free energy of the cations in the organic solvent relative to water noted in the present calculations shed additional light on this observation.

Solvation Structure in Liquid NMA. It has been shown previously that the hydration structure of alkali and halide ions from the Drude polarizable model agree well with available experimental data and *ab initio* results.[34,60,81] Figure 2 shows the radial distribution function (RDF) of the solvent oxygen atoms around the cations and the solvent polar hydrogen around the anion as well as the coordination number distributions. The ion coordination numbers in liquid NMA were calculated by integrating the corresponding RDF, taken as the outer limit of the first solvation shell (4.0 Å). The calculated coordination numbers from the polarizable Drude model are 5.2, 4.1, and 4.1 for K^+, Na^+ and Cl^-, respectively. The corresponding values calculated from the PARAM27/NBFIX model are 5.8, 5.4, and 5.3. Unsurprisingly, the coordination numbers are considerably smaller with the Drude polarizable force field than with the nonpolarizable PARAM27/NBFIX force field. While these results are consistent with numerous studies that have considered the effect of induced polarization,[28,29,31] there are no experimental data on the coordination number of ions solvated in liquid NMA available to assess those results. To further characterize the solvation structure of K^+ and Na^+ in liquid NMA in the absence of experimental data, *ab initio* DFT/MD simulations were carried out. The results, shown in Figure 2, provide additional force field-independent target information that can be used to assess the accuracy of the current models.

The average coordination number of K^+ calculated from the DFT/MD simulation is 5.0, in good accord with the value of 5.2 obtained from the Drude polarizable force field. Similarly, the average coordination number of Na^+ from the DFT/MD simulation is 4.0, also in very good agreement with the value of 4.1 from the Drude polarizable force field. The position of the first peak in the ion−NMA RDF of Na^+ and K^+ are consistent with the optimized distances from *ab initio* calculations reported in Table 3. For Na^+, the first peak in the ion−NMA RDF is located around 2.35−2.40 Å, while it is located at 2.40 Å in the simulations based on the Drude polarizable model. For K^+, the first peak of the RDF is located around 2.75 Å, the same as that from the simulations based on the Drude polarizable model. For both K^+ and Na^+, the first peaks in this radial distribution are slightly more diffuse than those from the fixed-charge and Drude polarizable models. A

(132) Peter, C.; Oostenbrink, C.; van Dorp, A.; van Gunsteren, W. F. *J. Chem. Phys.* **2004**, *120*, 2652–2661.
(133) Roux, B. *Acc. Chem. Res.* **2002**, *35*, 366–375.
(134) Flaschka, H.; Barnard, A. J. *Adv. Anal. Chem. Instrum.* **1960**, *1*, 1–117.

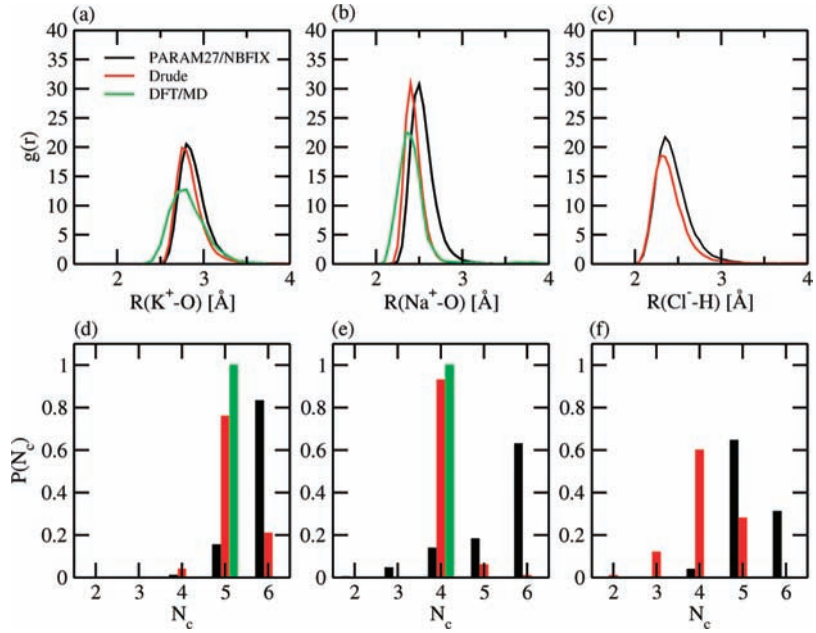

Figure 2. Radial distribution functions (RDFs) of solvent around the ions (a−c) and the coordination number distribution (d−f). (a) RDF of O−K^+. (b) RDF of O−Na^+. (c) RDF of H−Cl^-. (d) Coordination number (N_c) of K^+ in liquid NMA. (e) Coordination number (N_c) of Na^+ in liquid NMA. (f) Coordination number (N_c) of Cl^- in liquid NMA.

similar observation was previously made for K^+ solvated in liquid water.[34] One explanation is that the repulsive core is harsher in the classical models than in the DFT/MD simulation due to the utilization of the LJ potential. Alternatively, it is possible that the broader peak reflects the absence of van der Waals attractive dispersion, generally lacking or underestimated in DFT.[34] The coordination probability distribution $P(N)$ is also shown in Figure 2 (bottom). For K^+, the probability distribution $P(N)$ from the DFT/MD simulation is markedly centered on a single coordination state, with five NMA coordinating the cation. The same value dominates the coordination structure extracted from the MD simulation based on the polarizable model, although other coordination states are also present with a lower probability. For Na^+, the coordination probability distribution from the DFT/MD indicates that the cation is coordinated by four NMA molecules, with other coordination states visited infrequently in the simulations based on the polarizable Drude model. Examination of the time evolution of the coordination state in the simulations based on the polarizable model suggests that those infrequent coordination states, $N = 6$ for K^+ and $N = 5$ for Na^+, are not sampled completely in the short DFT/MD simulations.

Ion Selectivity in Small Clusters. The ion selectivity displayed by confined clusters comprising a small number of coordinating ligands allowed to fluctuate freely within a small volume is of great interest. Such reduced models offer a simplified representation of flexible protein binding sites and have been used in a number of studies of ion selectivity in biological systems.[84,102,135−139] Here, the relative free energy of Na^+ and K^+ in reduced models formed by NMA or water molecules is calculated with both nonpolarizable and polarizable models. The

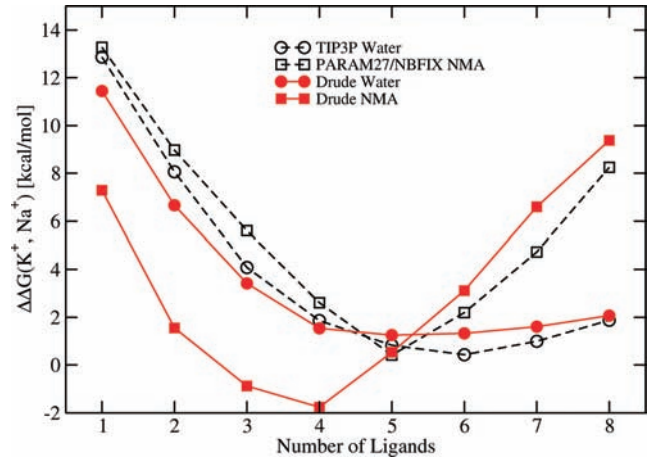

Figure 3. Solvation in the reduced models of one to eight ligands. Relative K^+ and Na^+ free energy of hydration in the gas phase as a function of the number of ligands in the cluster from simulations with both nonpolarizable and polarizable force fields.

results, shown in Figure 3, help further contrast the key features of ion solvation by NMA compared to water.

With water, the nonpolarizable and Drude models give consistent results for clusters of one to eight water molecules. This observation is in agreement with previous results.[102] The good accord explains, in part, why it has been possible to design nonpolarizable models to simulate ions in liquid water that are relatively accurate.[21] With ion solvation in NMA, the situation becomes more complex. As shown in Figure 3, the nonpolarizable force field is able to reproduce the relative free energy for models comprising five or more NMA molecules but fails when the cation is coordinated by only four or fewer NMA molecules. This failure is consistent with the known limitations of the nonpolarizable force field.[18]

The results given in Figure 3 reveal an intriguing feature displayed by the reduced models. There is an extremely sharp variation in the free energy governing the Na^+/K^+ selectivity

(135) Noskov, S. Y.; Roux, B. *Biophys. Chem.* **2006**, *124*, 279–291.
(136) Varma, S.; Rempe, S. B. *Biophys. J.* **2007**, *93*, 1093–1099.
(137) Thomas, M.; Jayatilaka, D.; Corry, B. *Biophys. J.* **2007**, *93*, 2635–2643.
(138) Bostick, D. L.; Brooks, C. L. *Proc. Natl. Acad. Sci. U.S.A.* **2007**, *104*, 9260–9265.
(139) Varma, S.; Rempe, S. B. *J. Am. Chem. Soc.* **2008**, *130*, 15405–15419.

as a function of the number of ligands in the reduced model. With four ligands, the calculated $\Delta\Delta G$ is -2 kcal/mol, rising by almost 3 kcal/mol for each added ligand for a total of 9 kcal/mol with eight NMA molecules. As a result, the reduced model with four NMA molecules is selective for Na^+, but is selective for K^+ when there are six or more NMA molecules. In contrast, the changes in the free energy governing the Na^+/K^+ selectivity in a reduced water model are much smaller. The $\Delta\Delta G$ is 0 kcal/mol with four water molecules, increasing gently to about 2 kcal/mol with eight water molecules. These results point to the extreme sensitivity of cation solvation by NMA with respect to the number of available ligands. They also indicate that considerations based on the coordination states of Na^+ and K^+ in liquid water would be expected to provide a poor representation the relative free energies of those ions in a flexible protein binding site comprising only backbone carbonyl ligands.[102,138] The difference between water and NMA directly reflects the effect of ligand−ligand repulsion, which varies roughly with the square of the dipole. Because the dipole moments of water and NMA differ almost by a factor of 2, the ligand−ligand repulsion is roughly 4 times larger with NMA than with water. Moreover, induced polarization amplifies this trend further, the molecular polarizability of NMA being considerably larger than that of water.[84] The impact of ligand−ligand repulsion is also reflected in the variations in the ion-oxygen distances. For both Na^+ and K^+, the distance between the ion and the oxygen ligand is smaller with one NMA molecule than with one water molecule. There is a crossover around 4−5 ligands, beyond which the ion−ligand distance become larger with NMA than with water. The ion−ligand distance starts to rise even more sharply with six or more ligands. These results help explain why both the type and the number of ligands play key roles in ion selectivity of flexible protein binding sites.[84,102,135]

Summary

We have carried out a combined experimental and computational study of ion interactions with NMA, which was used as a model system representing the amide group of proteins. The solubilities of KCl and NaCl in liquid NMA were measured, and the solvation free energies of the neutral salts were derived. A polarizable force field based on the classical Drude oscillator capable of capturing the complex electrostatic response of NMA to its environment was developed based on *ab initio* calculations to match experimental solvation free energies. The good agreement for the properties in both the gas phase and the condensed phase suggests that the current polarizable force field should be capable of describing with sufficient accuracy the K^+/Na^+ selectivity in membrane channels providing a permeation pathway lined by backbone carbonyl groups. The present effort provides a starting point for accurate computational studies aimed at characterizing various processes involving the binding of ions to proteins based on a force field taking into account induced polarization effects explicitly.

Acknowledgment. Financial support from the collaborative NIH Grant (GM-70971) to O.S.A., B.R., and R.K. is acknowledged. Additional support from the NIH Grant GM-72558 (B.R. and H.Y.) is also acknowledged. H.Y. thanks Dr. Ed Harder and Dr. Chris Rowley for helpful discussions.

Supporting Information Available: The parameters for the final models in this work and complete refs 9, 15, 85, and 106. This material is available free of charge via the Internet at http://pubs.acs.org.

JA103270W